A 2D Model of Induction Machine Dedicated to faults Detection– Extension of the Modified Winding Function

A. Ghoggal [1], S. E. Zouzou [2], A. Aboubou [2], M. Sahraoui [2].

Laboratoire de Génie Electrique
Département d'Electrotechnique
Université Mohamed Khider
B P.145, Biskra - Algérie.

[1] *ghoetudes@yahoo.fr*

***Abstract* – This paper treats mainly the modeling of induction machine inductances taking into account all the space harmonics, and with introduction of the effects of skewing rotor bars and linear rise of MMF across the slot. The model is established initially in the case of symetric machine, which corresponds to the case of a constant air-gap, then in the other case where the machine can present a static or dynamic, axial or radial eccentricity. This objective would be achieved by exploiting an extension in 2-D of the modified winding function approach (MWFA). It should be noted that this work gives a great number of results with consequently less explanation. It is of course our first aim; this can be noticed by a reader already leaning on the subject.**

***Index Terms* –- Induction machines, inductance, MWFA, spaces harmonics, skew.**

I. INTRODUCTION

The multiple coupled circuit, defined in the aim of approaching the real structure of the rotor cage, supposes that this one gathers a number of loops forming a polyphase winding, each loop consists of two adjacent bars and the two portions of the end ring which connect them [1]. Such a structure was used with profit in the diagnosis of the induction machine. Several studies were carried out in this axis, and made possible to reveal some phenomena rising from a defect, such as appearance of higher or lower sideband frequencies than the stator frequency in the spectral analysis of the line currents, torque, speed and power. Some papers supposes a perfect distribution of the MMF in the air-gap, others adopt models taking into account the real distribution of machine's windings [2], in particular with the implication of winding function, then, MWFA [3], where it is possible to detect some phenomena accompanying a probable eccentricity. And finally, the introduction of the axial dimension [4],[5]. The model is thus ready to define inductances of a machine taking into account the skew of the slots, and which can be extended to the study of other types of axial asymmetries, namely, the axial eccentricities.

In this work, a 2-D model of the induction machine will be approached while focusing the study on its first aim; the modeling of induction machine with non-sinusoidal distribution of the stator winding, and non-uniformity of the air gap. Simulation results as well as comments will be exposed.

II. A 2-D PRESENTATION OF THE MODIFIED WINDING FUNCTION APPROACH

To formulate the problem, we refer to Fig. 1 which gathers two cylindrical masses separated by an air-gap, one of it hollow and represent the stator, and the other represents the rotor. Given *abcda* an arbitrary contour definite in comparison to a reference of phase fixed on the stator, to an axial reference and to the mecanical position of the rotor measured by respecting a fixed stator reference. For a position θ_r of the rotor, and at $\varphi_0 = 0$ and $z_0 = 0$ are the points *a* and *b*, and at φ and *z* are *c and d*. On another side, *a* and *d* are located on the stator inner surface, and *b* and c on the rotor external surface.

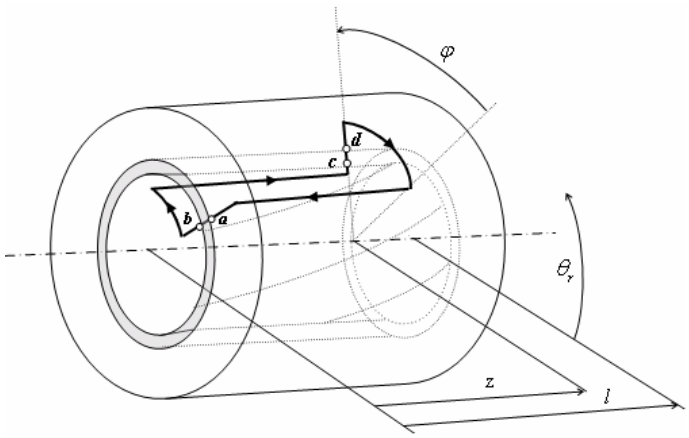

Fig. 1. Elementary induction machine

Let us take again the same stages of [3] but with the utilization of the axial dimension. Thus, according to the Gauss's law, the integral of the magnetic flux density on closed surface S of a cylindrical volume defined in comparison to the average radius of the air-gap *r* is null:

$$\oint_S \mathbf{B}\, ds = 0 . \qquad (1)$$

By definding , at any of coordinates (φ, z), the magnetic field intensity $\mathbf{H}$, the magnetomotive force F and the effective air-gap function g , such as $\mathbf{B} = \mu_0 \mathbf{H}$ and $\mathbf{H} = F / g$,

in this case (1) become

$$\mu_0 r \int_0^{2\pi}\int_0^{l} \frac{F(\varphi,z,\theta_r)}{g(\varphi,z,\theta_r)} dz d\varphi = 0, \quad (2)$$

where l is the effective length of the air-gap. On another side, and according to the Amper's law , it is possible to write

$$\oint_{abcda} \mathbf{H}(\varphi,z,\theta_r) dl = \int_{\Omega} J ds . \quad (3)$$

Ω is a surface enclosed by the closed path *abcda*, and J the current density. According to the MMF and the number of turns enclosed by the closed path *abcda* and traversed by the same current i , (3) can be written as

$$F_{ab}(0,0,\theta_r) + F_{bc} + F_{cd}(\varphi,z,\theta_r) + F_{da} = n(\varphi,z,\theta_r) i , \quad (4)$$

where $n(\varphi,z,\theta_r)$ is called the 2-D spatial winding distribution [5], or the 2-D turns function.

By considering an infinite permeability of iron, F_{bc} and F_{da} are null, the substitution of these values in (4) gives

$$F_{cd}(\varphi,z,\theta_r) = n(\varphi,z,\theta_r) i - F_{ab}(0,0,\theta_r) . \quad (5)$$

By introducing the average value of the inverse air-gap function $\langle g^{-1}(\varphi,z,\theta_r)\rangle$ with

$$\langle g^{-1}(\varphi,z,\theta_r)\rangle = \frac{1}{2\pi}\int_0^{2\pi}\left[\frac{1}{l}\int_0^{l} g^{-1}(\varphi,z,\theta_r) dz\right] d\varphi , \quad (6)$$

and while exploiting (2) and (5), it will be possible to lead to the expression giving $F_{cd}(\varphi,z,\theta_r)$ such as

$$F_{cd}(\varphi,z,\theta_r) = n(\varphi,z,\theta_r) i - \frac{1}{2\pi\ l\langle g^{-1}(\varphi,z,\theta_r)\rangle}\int_0^{2\pi}\int_0^{l} n(\varphi,z,\theta_r) g^{-1}(\varphi,z,\theta_r) i dz d\varphi \quad (7)$$

The 2-D winding function can be obtained by dividing the members of (7) by *i*:

$$N(\varphi,z,\theta_r) = n(\varphi,z,\theta_r) - \frac{1}{2\pi\ l\langle g^{-1}(\varphi,z,\theta_r)\rangle}\int_0^{2\pi}\int_0^{l} n(\varphi,z,\theta_r) g^{-1}(\varphi,z,\theta_r) dz d\varphi \quad (8)$$

It is to be noticed that this new expression does not hold any restriction as for the axial uniformity, in particular in term of skewing slots and axial air-gap non uniformity.

III. CALCULATION OF INDUCTANCES

A. Machine with uniform air-gap

Firstly, supposing that the machine is symmetrical. The air-gap length g is reduced to g_0 which is the radial air-gap length in the case of no eccentricity. If F is the MMF distribution in the air-gap due to the current i_{A_i} flowing in an arbitrary coil A_i , and knowing that the elementary flux corresponding in the air-gap is measured in comparison to an elementary volume of section *ds* and length g_0 such as

$$d\phi = \mu_0 F g_0^{-1} ds , \quad (9)$$

the calculation of total flux returns to a calculation of double integral. By carrying out the change of variable $x = r\varphi$ and $x_r = r\theta_r$ it is as if the study referred to a reference with axes X and Z where it is possible to imagine a plane representation of the machine. It is clear that, in this case, x translate correctly the linear displacement along the arc corresponding to the angular opening φ. In the same way concerning x_r and θ_r.

Knowing that N is the MMF per unit of current, the expression giving the flux seen by all the turns of coil B_j of winding *B* due to i_{Ai} flowing in coil A_i will be reduced as

$$\phi_{BjAi} = \frac{\mu_0}{g_0}\int_{x_{1j}}^{x_{2j}}\int_{z_{1j}(x)}^{z_{2j}(x)} N_{Ai}(x,z,x_r) n_{Bj}(x,z,x_r) i_{Ai} dz dx. \quad (10)$$

That is due to the fact that by taking account the axial asymmetry, $n_{Bj}(x,z,x_r)$ will be defined so as to be able to translate the skew of the slots. In 2-D, it will be written in the following way:

$$n_{Bj}(x,z,x_r) = \begin{cases} w_{Bj} & x_{1j} < x < x_{2j}\ ,\ z_{1j}(x) < z(x) < z_{2j}(x), \\ 0 & \text{in the remaining interval} \end{cases} \quad (11)$$

where w_{Bj} is the number of turns of coil B_j . It is equal to 1 in the case of a rotor loop. Generally, the total flux ψ_{BA} relating to all coils composing winding A and B holds its general expression by integrating over the whole surface. And knowing that the mutual inductance L_{BA} is the flux ψ_{BA} per unit of current, yields

$$L_{BA}(x_r) = \frac{\mu_0}{g_0}\int_0^{2\pi r}\int_0^{l} N_A(x,z,x_r) n_B(x,z,x_r) dz dx . \quad (12)$$

Let us notice that a rearrangement of (12) makes possible to define an inductance defined per unit of length as described in [4]:

$$L_{BA}(x_r) = \int_0^{l} L'_{BA}(z,x_r) dz . \quad (13)$$

In the same way as [1], and according to the manner of connection of the coils translated by the sign in (14), this inductance can be obtained by summing all mutual inductances between the q and p coils of winding *A* and *B* respectly, such as:

$$L_{BA}(x_r) = \sum_{i=1}^{q} \sum_{j=1}^{p} \pm L_{B_j A_i}(x_r) \qquad (14)$$

B. Bars skewing

Fig. 2 depicts the passage of a rotor loop r_j under the field of a stator coil A_i . The skew is translated by the definition of z(x) in (10) which will be a function describing the uniform skew, or particularly, the case of spiral skew.

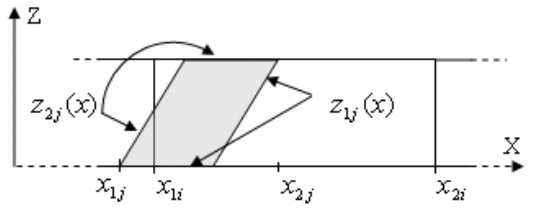

Fig. 2. Representation of the skew

Note that the pitch α_{Ai} of the coil A_i is defined in comparison to its sides placed at $x_{1i} = r.\varphi_{1i}$ and $x_{2i} = r.\varphi_{2i}$, and that the effect of linear rise of MMF across the slot is note represented in the figure.

C. Slot opening.

Let us examine the case of coil A_i with w_{Ai} turns placed in slots which, according to case's, can present an opening of width β according to the simple configuration considered. Fig. 3 shows the turns function of coil A_i if the slot opening is taken into account in the calculation of the resultant linear rise of MMF across the slot.

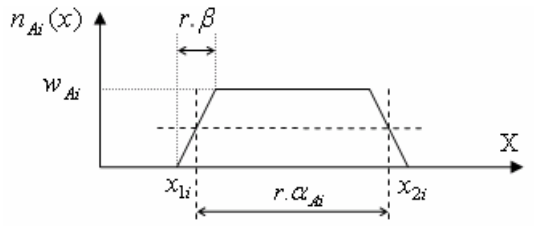

Fig. 3. Turns function of coil A_i

D. Machine with an eccentric rotor

Equation (12) takes its generalized form as:

$$L_{BA}(x_r) = \mu_0 \int_0^{2\pi r} \int_0^{l} N_A(x,z,x_r) n_B(x,z,x_r) g^{-1}(x,z,x_r) dz dx. \qquad (15)$$

With the use of (14) and (15), it will be possible to calculate all inductances of the machine if:

$g^{-1} = g^{-1}(x, x_r)$: Case of a purely radial eccentricity.

$g^{-1} = g^{-1}(x, z, x_r)$: The case where this eccentricity appears also along axis Z.

g^{-1} is giving by its general expression as follows:

$$g^{-1}(x,z,x_r) = \frac{1}{g_0(1 - \delta_s(z)\cos(x/r) - \delta_d(z)\cos((x - x_r)/r)}, \qquad (16)$$

where δ_s and δ_d are the amount of static and dynamic eccentricity respectly which are function of z. A numerical calculation makes possible to find the integral (15), however, an analytical resolution must call upon an approximated expression of g^{-1} by carrying out a development in Fourier series. A perfect result would be obtained while stopping at the third term, such as:

$$g^{-1}(x,z,x_r) \approx P_0(z) + P_1(z)\cos(x/r - \rho) + P_2(z)\cos(2(x/r - \rho)) \qquad (17)$$

ρ and coefficients P_0, P_1 and P_2 are calculated from $g_0, \delta_s(z), \delta_d(z)$ and θ_r like describing in [7]and [8]. It is to be recalled that for any winding *A* and *B*, equality $L_{AB} = L_{BA}$ is always checked [7], and that all was calculated compared to an average radius of the air-gap *r* in the case of no eccentricity, while admitting that the variations in the radius of the air-gap *R* due to the eccentricity are negligible in front of the radius itself, which is not the case concerning g , it is what can be translated as

$$\frac{R(x,z,x_r)}{g(x,z,x_r)} = \frac{r \pm \Delta R(x,z,x_r)}{g_0 \pm \Delta g(x,z,x_r)} \approx \frac{r}{g_0 \pm \Delta g(x,z,x_r)} \qquad (18)$$

IV. SIMULATION RESULTS

A. Machine with uniform air-gap.

The first induction machine studied in this paper is a three-phase, 4-pole motor [4], whose parameters appear in the Appendix, and the structure of the stator coils of Fig. 4, where only phase A is represented, and one of its coils numbered. Each circle represents the section of an elementary coil of *w* turns. A,B, and C are the three stator phases, and r_j the j^{th} rotor loop.

Fig. 4. Winding of stator phase A

Fig. 5 illustrates the functions which describe the mutual inductances L_{r1A} between the first stator phase A, and the first rotor loop, in the four cases considered, without and with taking into account the slots opening and the skewing of rotor bares. A rotor loop is regarded as being a coil with one turn. Note that the mutual inductance beteween phase and the seconde rotor loop is the same as giving in Fig. 5, but shifted to the left by $2\pi / Nb$. As for the other inductances, L_{r1B} and L_{r1C} are identically reproduced, but shifted to the right by $\pi / 3$. The mechanical angle of

skewing of the rotor bars is $\gamma = \pi/12$ rad, which is selected equal to one stator slot pitch [6], and the width of slot opening $\beta = \pi/24$. In each figure, the function whose maximum value is most significant, represents the first derivative of the curve of mutual inductance L_{r1A}.

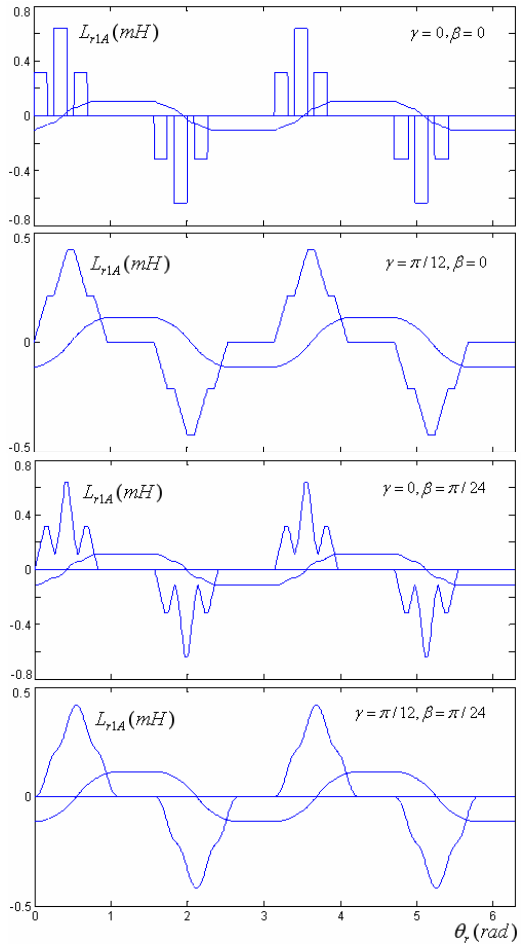

Fig. 5. Mutual inductance between stator phase A and rotor loop r_1

As for the self and the mutual inductances between windings of the same frame (stator or rotor), it should be noted that those are not affected by the effect of skewing, however, a variation in the values of the stator inductances is noted, and it is due to the taking into account of the linear rise of MMF across the slot (Table I).

TABLE I
STATOR INDUCTANCES

	$L_A(H)$	$L_{AB}(H)$
$\beta = 0$	*0.1198*	*-0.0532*
$\beta = \pi/24$	*0.1165*	*-0.0529*

B. Machine with an eccentric rotor

1) Radial eccentricity: The second specific induction motor studied is a three-phase, 11kw, 50Hz, 4-pole motor, having four coils per phase group, eight coils per phase, series connected [10]. The others parameters are given in the Appendix. Figs. 6,7,8,9,10 and 11show the results of simulation for different degrees of eccentricity, and with three terms P_0, P_1 and P_2 used in the development of g^{-1}.

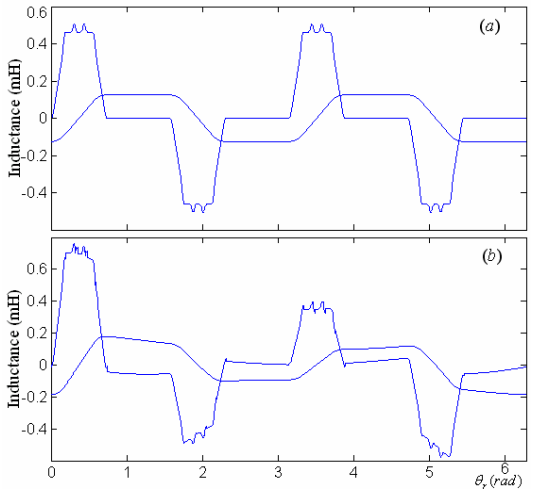

Fig. 6. L_{r1A} and $\frac{dL_{r1A}}{d\theta_r}$ a) symetric machine, b) δ_s =35%, δ_d =0

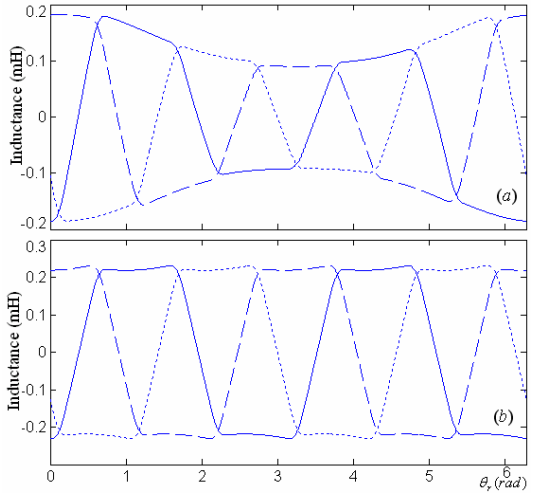

Fig. 7. Mutual inductances $L_{r1A}, L_{r1B}, L_{r1C}$ for:
a) δ_s = 35% , δ_d = 0 b) δ_s = 0% , δ_d = 50%

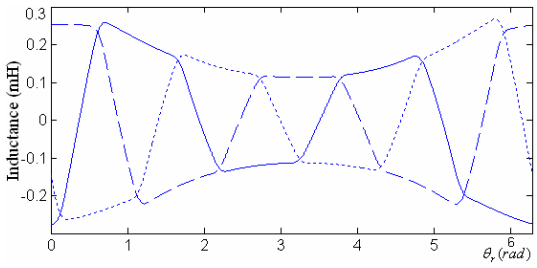

Fig. 8. $L_{r1A}, L_{r1B}, L_{r1C}$ case of mixed eccentricity of δ_s = 35% and δ_d = 25%.

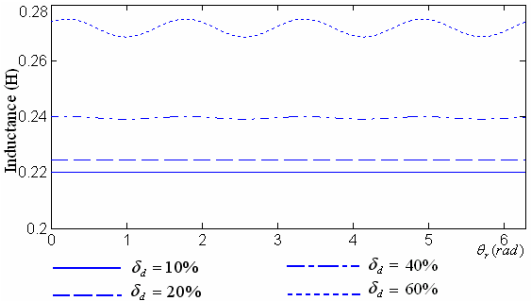

Fig. 9. Self inductance of phase A for different degrees of dynamic eccentricity

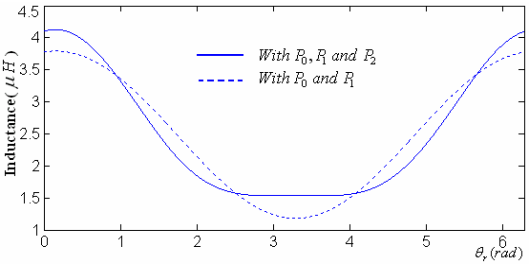

Fig. 10. Self inductance of rotor loop r_1 for 50% of static eccentricity

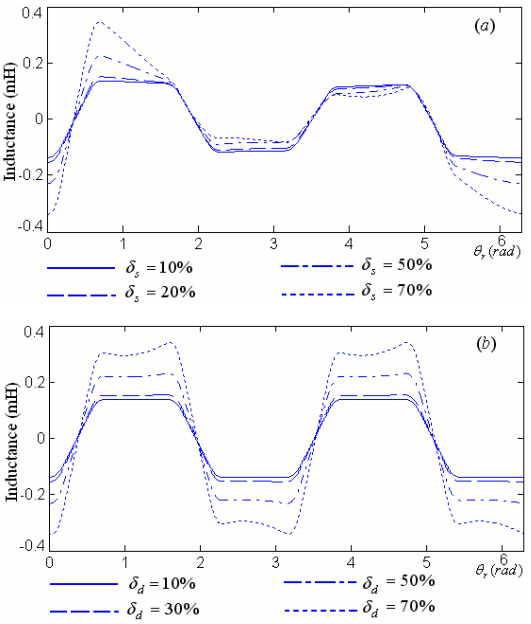

Fig. 11. Mutual inductance L_{r1A} for different degrees of eccentricity, a) Satic eccentricity , b) Dynamic eccentricity.

2) Axial eccentricity: To examine the case of the static eccentricity, the expression of $\delta_s(z)$ must be defined. According to Fig. 12 showing the external diameter of the rotor and the internal diameter of the stator with exaggeration in the representation of the air-gap, $\delta_s(z)$ can be written as

$$\delta_s(z) = \delta_{s0}.(1-\frac{z}{L}). \tag{19}$$

As presented in Fig. 12, the minimum air-gap for $z=0$ is supposed at $\varphi = 0$ along the vertical axis. The minimal air-gap has a fixed angular position for the different values of z inferior than L, but its value depends on z.

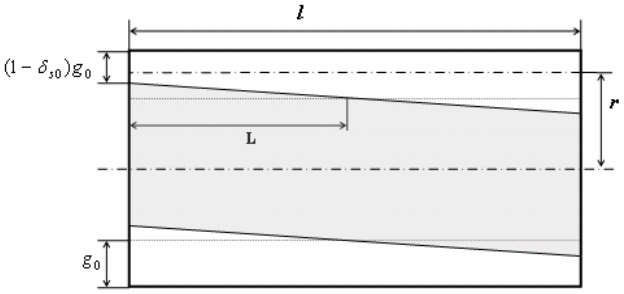

Fig. 12. Illustration of the axial eccentricity.

On another side, if the perfectly concentric section of the rotor corresponds to z =L, in this case, in the modeling of the eccentricity, L must be selected superior than a certain value guaranteeing the existence of an air-gap with $g(x,z,x_r) \neq 0$ along the rotor length. For $L \to +\infty$, as a result $\delta_s(z) \to \delta_{s0}$, and the study returns to the case of the purely radial eccentricity. Fig. 13 chows the mutual inductance between stator phase A and the first rotor loop with rotor position when $\delta_{s0} = 70\%$ and $L = l/2$.

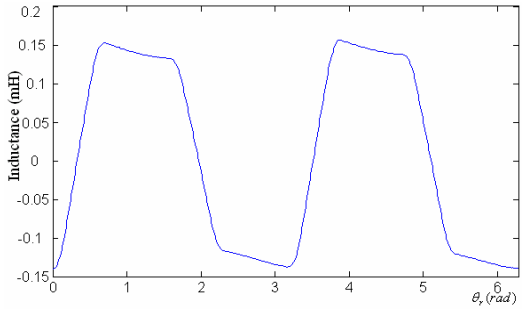

Fig. 13. L_{r1A} for $\delta_{s0} = 70\%$ and $L = l/2$.

C. Operation under condition of mixed eccentricity.

Knowing that the cage can be viewed as identical and equally speaced rotor loops, it is possible to establish voltage equations of stator and rotor loops as [1],[2]:

$$[U_s] = [R_s][I_s] + \frac{d[\psi_s]}{dt}, \tag{20}$$

$$[\mathbf{0}] = [R_r][I_r] + \frac{d[\psi_r]}{dt}, \tag{21}$$

$$[\psi_s] = [L_{ss}][I_s] + [L_{sr}][I_r], \tag{22}$$

$$[\psi_r] = [L_{rs}][I_s] + [L_{rr}][I_r]. \tag{23}$$

The vector $[U_s]$ corresponds to the stator voltages, $[I_s]$ and $[I_r]$ to the stator and rotor currents. m is the number of stator phases and N_b the number of rotor bars. $[R_s]$ is an m dimentional diagonal matrix, $[L_{ss}]$ is an $m \times m$ symetric

matrix, $[L_{sr}]$ is an $m\times(N_b+1)$ matrix, and $[R_r]$ and $[L_{rr}]$ are $(N_b+1)\times(N_b+1)$ matrix. Adding to these equations the mechanical and electromagnetic torque equations:

$$C_e - C_r = J_r \frac{d\omega_r}{dt} \quad , \quad C_e = \left(\frac{dW_{co}}{d\theta_r}\right)\Bigg|_{(I_s, I_r = \text{constant})} , \quad (24)$$

and

$$W_{co} = \frac{1}{2}([I_s]^T[L_{ss}][I_s] + [I_s]^T[L_{sr}][I_r] + [I_r]^T[L_{rr}][I_r] + [I_r]^T[L_{rs}][I_s]), \quad (25)$$

where W_{co} is the coenergy, C_e the electromagnetic torque , C_r the load torque, J_r the rotor load inertia, and ω_r the mechanical speed of the rotor. Fig. 14 shows the simulation result of the operation of machine (2) under conditions of mixed eccentricity of $\delta_s = 40\%$, $\delta_d = 20\%$.

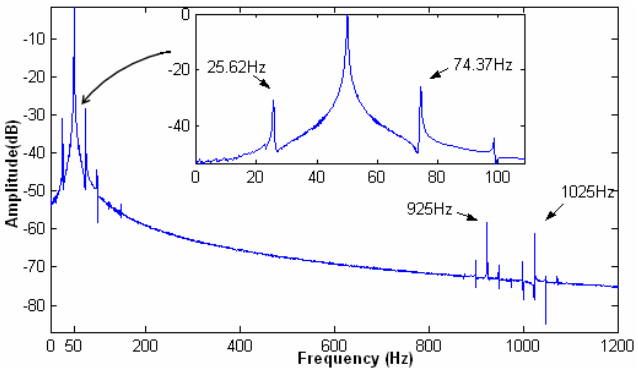

Fig. 14. Stator curent spectra with mixed eccentriciry condition, δ_s =40% , δ_d =20% , slip =2.5%.

In the spectra of Fig. 14 relating to the current of the first stator phase, it is possible to see the first components wich are function of static eccentricity. This result is derived from the general equation given in [8], and described by

$$f_{slot+ecc} = f_s \cdot (\frac{N_b}{p}(1-s) \pm 1), \quad (26)$$

f_s represents the mains frequency and s the slip. In the zoom appear the low frequency components near the fundamental. This result is as predicted in [9] and described by

$$f_{ecc} = f_s \cdot (1 \pm (1-s)/p). \quad (27)$$

V. CONCLUSION

In this work, the bases of MWFA were presented with introduction of the axial dimension. It was applied in the calculation of the induction machine inductances with, initially, taking into account of all the space harmonics. And secondly, taking into account of the effects generated by the skew and linear rise of MMF across the slots. Then finally, the modeling in the air gap eccentricity conditions, in the differents cases of eccentricity considered, static, dynamic, radial and axial. For that, a simulation tools was established. The obtained results were compared with the final results of [4] and [10], and a perfect agreement was noted, but this new technique prove less complicated to be translated into algorithm than that given by the expression of inductance per unit of length as described in [4]. It is advisable to integrate the effect of saturation, and to envisage operation under other faults conditions. It is what constitutes our work perspective.

APPENDIX

Machines Parameters : - Machine (1) : $g_0 = 0.0006m$, $r = 0.066m$, $l = 0.115m$, $w = 20$, Nb =36 , Ne =24. - Machine (2) : $g_0 = 0.0008m$, $r = 0.082m$, $l = 0.11m$, $w = 28$, Nb=40 , Ne=48 , L_b =95nH , L_e =18nH, $R_s = 1.75\Omega$, $R_b = 31\mu\Omega$, $R_e = 2.2\mu\Omega$, $J_r = 0.0754 kgm^2$, $\gamma = \pi/20 rad$, $\beta = \pi/86 rad$.

REFERENCES

[1] X. Luo, Y. Liao, H.A. Toliyat, A. El-Antably, and T.A. Lipo, "Multiple coupled circuit modeling of induction machines," *IEEE Trans. Industry Applications*, vol. 31,no. 2, pp. 311-318, Mar./Apr. 1995.

[2] H. A Toliyat, T.A Lipo,"Transient analyse of induction machines under stator, rotor bar and end ring faults, "*IEEE Trans. Energy Conversion*, vol. 10, no. 2, pp. 241-247, June 1995.

[3] N.A. Al-Nuaim and H.A. Toliyat, "A novel method for modeling dynamic air-gap eccentricity in synchronous machines based on modified winding function theory," *IEEE Trans. Energy Conversion*, vol. 13, no. 2, pp. 156-162, June 1998.

[4] M. G. Joksimovic, D. M. Durovic and A. B. Obradovic, "Skew and linear rise of MMF across slot modeling-Winding function approach," *IEEE Trans. Energy Conversion*, Vol. 14, no. 3, pp. 315-320, Sept. 1999.

[5] G.Bossio, C.D. Angelo, J.Solsona, G. García and MI. Valla, "A 2-D Model of the induction machine : Extension of the modified winding function approach," *IEEE Trans.Energy Convertion*, vol. 19, no. 1, pp. 144-150, Mar. 2004.

[6] M. Liwschitz and L. Maret, Calcul des machines électriques, Bibliothèque de l'ingénieur, Editions SPES Lausanne: 1970.

[7] J. Faiz and I. Tabatabaei, "Extension of winding function theory for nonuniform air gap in electric machinery, "*IEEE Trans. Magnetics*, vol. 38, no. 6, pp. 3654-3657, Nov. 2002.

[8] S. Nandi, R.M. Bharadwaj and H.A. Toliyat, " Performance analyse of three-phase induction motor under mixed eccentricity condition," *IEEE Trans. Energy Conversion*, vol. 17, no. 3, pp. 392-399, Sept. 2002.

[9] D.G. Dorrell, W.T. Thomson and S.Roach, "Analyse of airgap signals as function of combination static and dynamic airgap eccentricity in 3-phase induction motors," *IEEE Trans. Industry Applications*, vol. 33, no. 1, pp. 24-34, Jan./Feb. 1997.

[10] M. G. Joksimovic, D. M. Durovic, J. Penman and N. Arthur," Dynamic simulation of dynamic eccentricity in induction machines-Winding function approach," *IEEE Trans. Energy Conversion*, vol. 15, no. 2 , pp. 143-148, June 2000.